AIP | Applied Physics Letters

Electronic-resonance-enhanced coherent anti-Stokes Raman spectroscopy of nitric oxide

Sherif F. Hanna, Waruna D. Kulatilaka, Zane Arp, Tomas Opatrný, Marlan O. Scully, Joel P. Kuehner, and Robert P. Lucht

Citation: Applied Physics Letters **83**, 1887 (2003); doi: 10.1063/1.1604947
View online: http://dx.doi.org/10.1063/1.1604947
View Table of Contents: http://scitation.aip.org/content/aip/journal/apl/83/9?ver=pdfcov
Published by the AIP Publishing

Electronic-resonance-enhanced coherent anti-Stokes Raman spectroscopy of nitric oxide

Sherif F. Hanna and Waruna D. Kulatilaka
Department of Mechanical Engineering, Texas A&M University, College Station, Texas 77843

Zane Arp
Department of Chemistry, Texas A&M University, College Station, Texas 77843

Tomas Opatrný and Marlan O. Scully[a)]
Department of Physics, Texas A&M University, College Station, Texas 77843

Joel P. Kuehner
Department of Mechanical and Industrial Engineering, University of Illinois, Urbana, Illinois 61801

Robert P. Lucht[b)]
School of Mechanical Engineering, Purdue University, West Lafayette, Indiana 47907

(Received 17 February 2003; accepted 27 June 2003)

A dual-pump, electronic-resonance-enhanced coherent anti-Stokes Raman spectroscopy (CARS) technique for the measurement of minor species concentrations has been demonstrated. The frequency difference between a visible Raman pump beam and Stokes beam is tuned to a vibrational *Q*-branch Raman resonance of nitric oxide (NO) to create a Raman polarization in the medium. The second pump beam is tuned into resonance with rotational transitions in the (1,0) band of the $A^2\Sigma^+ - X^2\Pi$ electronic transition at 236 nm, and the CARS signal is thus resonant with transitions in the (0,0) band. We observe significant resonant enhancement of the NO CARS signal and have obtained good agreement between calculated and experimental spectra. © *2003 American Institute of Physics.* [DOI: 10.1063/1.1604947]

Electronic-resonance-enhanced (ERE) coherent anti-Stokes Raman spectroscopy (CARS) measurements of nitric oxide (NO) were performed using a three-laser CARS technique. The technique that we have demonstrated is a variant of the dual-pump CARS technique developed for the simultaneous detection of two species.[1,2] An energy level schematic for the technique is shown in Fig. 1. The first pump and Stokes beams are visible laser beams with frequencies far from resonance with the $A^2\Sigma^+ - X^2\Pi$ electronic transition. The second pump beam at frequency ω_3 is in or near electronic resonance. This wide separation of the frequencies ω_1 and ω_3 of the two pump beams distinguishes our technique from previous ERE CARS experiments,[3–5] which were performed with the same laser frequency for both pump beams, and with both the pump and Stokes beams at or near electronic resonance. In some cases, three laser frequencies, all in or near electronic resonance, were used in ERE CARS experiments.[6,7]

The pump source for the ω_1 pump beam was a Continuum model 9010 injection-seeded, *Q*-switched Nd:yttritium–aluminum–garnet (YAG) laser with a repetition rate of 10 Hz, pulse length of approximately 7 ns, and pulse energy for the 532 nm output of approximately 750 mJ. The 532 nm output was also used to pump a Continuum model ND6000 narrowband, tunable dye laser to produce the Stokes beam (ω_2) at a wavelength near 590 nm with a frequency bandwidth of approximately 0.08 cm^{-1}. The 355 nm third-harmonic output of a Continuum model 8010 Nd:YAG laser was used to pump a second Continuum model ND6000 dye laser to produce tunable laser radiation at a wavelength of 472 nm. The 472 nm output of the dye laser was frequency doubled to 236 nm using an INRAD Autotracker III with a beta barium borate (β-BBO) crystal to produce the pump beam at frequency ω_3 with an estimated frequency bandwidth of 0.2–0.3 cm^{-1}.

The CARS signal was generated using a three-dimensionally phase-matched arrangement. The pulse energies for the 532, 590, and 236 nm beams at the CARS probe volume were typically 30, 20, and 1 mJ, respectively. The CARS focusing lens had a focal length of 300 mm. After

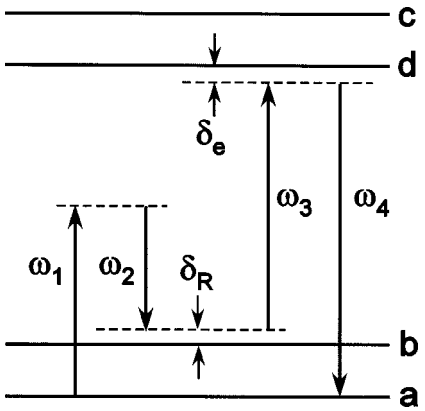

FIG. 1. Energy level schematic diagram of the dual-pump ERE CARS process.

[a)]Also at: Department of Chemistry, Princeton University, Princeton, New Jersey 08544.

[b)]Author to whom correspondence should be addressed; electronic mail: lucht@purdue.edu

passing through the ERE CARS probe volume, the pump, Stokes, and CARS signal beams were recollimated using a 300 mm focal length lens. The 532 nm pump and Stokes beams were directed into beam dumps. The 236 nm pump beam was directed into a pyroelectric Joulemeter to measure the pulse energy. The ERE CARS signal was directed through apertures and four 45° incidence, 215 nm dielectric mirrors. The 215 nm mirrors were used at 0° incidence and had approximately 70% transmittance at 226 nm but less than 1% transmittance at 236 nm. These mirrors served as spectral filters and reduced significantly the background from the 236 nm scattered light. The ERE CARS signal beam was then focused onto the entrance slit of a 0.5 m spectrometer, and a solar-blind photomultiplier was used to detect the 226 nm ERE CARS signal. The ERE CARS signals and the ultraviolet pulse energies were recorded on a shot-by-shot basis using gated integrators while either the Stokes dye laser or the ultraviolet pump dye laser was scanned under computer control.

Polarization techniques were used to suppress the nonresonant four-wave mixing background signal.[8] Both the 532 nm pump beam and the Stokes beams were linearly polarized with the polarization axis at 60° to the vertical. The ultraviolet pump beam was vertically polarized. For this polarization arrangement the resonant CARS signal is generated with a nearly vertical polarization, while the nonresonant background is linearly polarized at 30° to the vertical. An α-BBO polarizer was placed in the signal channel with its transmission axis perpendicular to the polarization of the nonresonant background. This resulted in a drastic reduction in the intensity of the nonresonant background. The ERE CARS signal intensity was also reduced, but the signal-to-noise ratio for the ERE CARS signal was significantly increased.

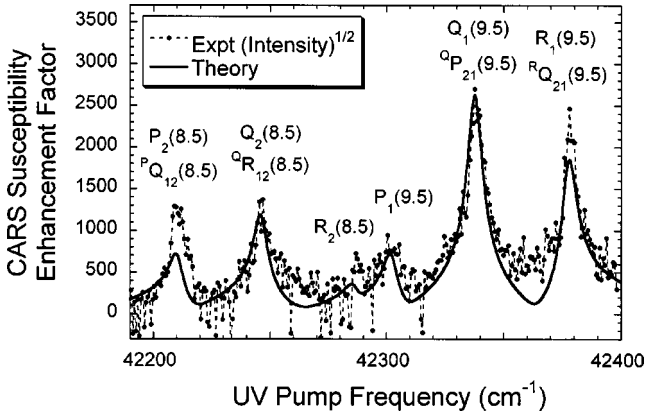

FIG. 2. ERE CARS spectra obtained by scanning the ultraviolet pump beam with the Stokes beam frequency fixed at 1874.35 cm^{-1}. The NO concentration was 1000 ppm and the cell pressure was 13.0 kPa.

The results of a spectral scan of the ultraviolet pump beam frequency ω_3 at fixed Raman shift $\omega_1-\omega_2$ is shown in Fig. 2. The scan was performed on a mixture of 1000 ppm of NO in a buffer gas of N_2. The cell was at room temperature, approximately 300 K, and at a pressure of 13.0 kPa. The spectrum was modeled using a perturbative ERE CARS analysis.[3–7] The basic equation for the CARS susceptibility is given by

$$\chi_{\mathrm{CARS}}(\omega_4:\omega_1,-\omega_2,\omega_3)=\frac{N}{\hbar^3}\sum_{a,b,c,d}\left(\left[\frac{1}{\omega_{ba}-(\omega_1-\omega_2)-i\Gamma_{ba}}\right]\left[\frac{\mu_{4ad}\mu_{3db}}{\omega_{da}-\omega_4-i\Gamma_{da}}\right]\left\{\left[\frac{\rho_{aa}^{(0)}\mu_{1bc}\mu_{2ca}}{\omega_{ca}+\omega_2-i\Gamma_{ca}}\right]+\left[\frac{\rho_{aa}^{(0)}\mu_{2bc}\mu_{1ca}}{\omega_{ca}-\omega_1-i\Gamma_{ca}}\right]-\left[\frac{\rho_{bb}^{(0)}\mu_{2bc}\mu_{1ca}}{\omega_{cb}-\omega_2+i\Gamma_{cb}}\right]-\left[\frac{\rho_{bb}^{(0)}\mu_{1bc}\mu_{2ca}}{\omega_{cb}+\omega_1+i\Gamma_{cb}}\right]\right\}\right),$$

where $\chi_{\mathrm{CARS}}(\omega_4:\omega_1,-\omega_2,\omega_3)$ is the CARS susceptibility, $\mu_{1ac}=\boldsymbol{\mu}_{ac}\cdot\hat{e}_1$, where $\boldsymbol{\mu}_{ac}$ (C m) is the electric dipole moment matrix element for states a and c, $\hat{e}_1$ is the unit polarization vector for the electric field of pump 1, $\rho_{aa}^{(0)}$ is the initial population of state a, N is the total number density (m^{-3}) of resonant molecules, $\hbar$ is Planck's constant (J s), Γ_{ab} is the dephasing rate (s^{-1}) for the electric dipole transition between states a and b, and other parameters are defined in a similar fashion. The Sandia CARS code[9] was modified for the ERE CARS calculations and the NO spectral data were obtained from the spectroscopic database code LIFBASE[10] and from previous high-resolution NO CARS measurements.[11,12] The square root of the CARS intensity is plotted in Fig. 2 versus the theoretical enhancement factor. The enhancement factor is the square root of the calculated CARS intensity for the ultraviolet pump frequency divided by square root of the calculated CARS intensity for $\lambda_3=532$ nm. As can be seen from Fig. 2, there is good agreement between theory and experiment and we observe an enhancement factor of nearly 2500 at the peak of the $Q_1(9.5)$ line. The spectral line assignments in Fig. 2 can be understood by examination of Fig. 3. The main-branch electronic resonances, $Q_1(9.5)$, $R_1(9.5)$, and $P_1(9.5)$ will be predominant in the spectrum when the Raman Q-branch transition between the $J=9.5=N+0.5$ levels in the (1,0) band in the $X^2\Pi$ state is probed. The occurrence of the $Q_2(8.5)$, $R_2(8.5)$, and $P_2(8.5)$ lines in the same scan indicates that the Raman Q-branch transition between the $J=8.5=N-0.5$ levels in the (1,0) band occurs at nearly the same Raman shift.

Comparison between theory and experiment is complicated by the noise in the spectrum resulting from the multimode frequency structure of the 236 and 590 nm beams. It is also complicated by the short lifetime of the LDS 490 laser dye that was used to produce the 472 nm beam, resulting in a continuous decrease in the 236 nm laser power over the course of the spectral scans. Despite this, we are able to reproduce the major spectral features of the data for a wide range of ultraviolet pump laser scans with fixed Stokes frequency, using only two constant frequency offset parameters for the ω_2 and ω_3 beams. There appears to be significant

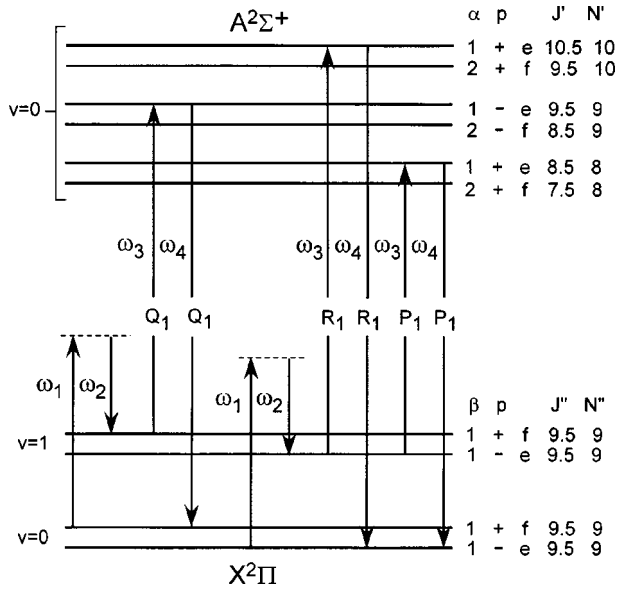

FIG. 3. ERE CARS energy level diagram specialized to the case where the Raman resonance frequency is tuned to the Q-branch resonances between the $J''=9.5$ in the (1,0) Raman band. The three main-branch transitions, $Q_1(9.5)$, $R_1(9.5)$, and $P_1(9.5)$, through which electronic resonance enhancement occurs are shown in the diagram; satellite transitions are not shown.

saturation or Stark broadening[13] of the ultraviolet transition, because it was necessary to increase the theoretical spectral width of the ultraviolet pump laser to a value of 6 cm^{-1} to obtain good agreement between the experimental and theoretical width of the resonance lines. This increase in ultraviolet pump spectral width decreased the theoretical susceptibility enhancement factor by more than a factor of 10. The intensity dependence of the NO ERE CARS spectrum will be investigated in detail in future studies. The use of high-resolution, single-mode Stokes and ultraviolet laser sources may lead to significantly lower detection limits.

Good agreement between theory and experiment was also achieved for spectra obtained when the Stokes laser was scanned. Signal-to-noise ratios in excess of 10 were obtained from mixtures of 100 ppm NO in N_2 buffer gas, as shown in Fig. 4. The combination of the polarization suppression of the nonresonant background and the electronic resonance enhancement results in a significant decrease in the CARS detection limit. Polarization CARS measurements of NO in plasmas have been reported by Doerk *et al.*[14] and by Pott *et al.*[15] Pott *et al.*[15] report a detection limit of 200 ppm NO at room temperature and atmospheric pressure, but in the published CARS spectrum for this condition the NO signal is just barely discernable from the background signal.

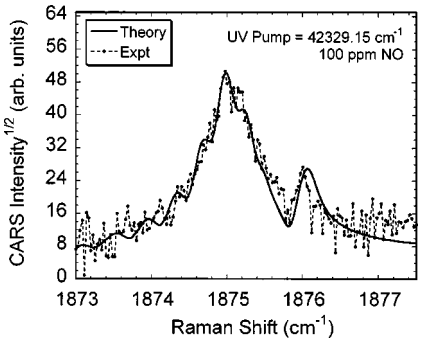

FIG. 4. ERE CARS spectra obtained by scanning the Stokes beam with the ultraviolet pump frequency fixed at 42 329.15 cm^{-1}. The NO concentration was 100 ppm and the cell pressure was 71.1 kPa.

We have demonstrated the detection of ERE CARS signals from NO in concentrations as low as 100 ppm. Spectral scans were obtained with a fixed Stokes frequency as the ultraviolet pump frequency was varied, and with a fixed ultraviolet pump frequency as the Stokes frequency was varied. Good agreement between theory and experiment was obtained for both these cases. The use of the dual-pump ERE CARS technique allows us to separate clearly the process by which the Raman coherence is induced in the medium from the ERE process where the Raman coherence is probed with a second pump beam. This separation simplifies considerably the theoretical modeling of the ERE CARS process, and may enable sensitive, selective detection of small polyatomic molecules in flames and plasmas. The successful implementation of the technique for NO is a very significant step towards ERE CARS detection of biological molecules of interest.[16]

This work was supported by the Defense Advanced Research Project Agency (DARPA), by the U.S. Dept. of Energy, Office of Basic Energy Sciences, Division of Chemical Sciences, Geosciences, and Biosciences, and by the U.S. Army Research Office.

[1] R. P. Lucht, Opt. Lett. **12**, 78 (1987).
[2] R. P. Lucht, V. N. Velur, C. D. Carter, K. D. Grinstead, Jr., J. R. Gord, P. M. Danehy, G. J. Fiechtner, and R. L. Farrow, AIAA J. **41**, 679 (2003).
[3] B. Attal-Trétout, O. O. Schnepp, and J.-P. E. Taran, Opt. Commun. **24**, 77 (1978).
[4] T. Doerk, P. Jauernik, S. Hädrich, B. Pfelzer, and J. Uhlenbusch, Opt. Commun. **118**, 637 (1995).
[5] T. Doerk, M. Hertl, B. Pfelzer, S. Hädrich, P. Jauernik, and J. Uhlenbusch, Appl. Phys. B: Lasers Opt. **B36**, 111 (1997).
[6] B. Attal-Trétout, S. C. Schmidt, E. Crété, P. Dumas, and J.-P. E. Taran, J. Quant. Spectrosc. Radiat. Transf. **43**, 351 (1990).
[7] B. Attal-Trétout, P. Berlemont, and J.-P. E. Taran, Mol. Phys. **70**, 1 (1990).
[8] L. A. Rahn, L. J. Zych, and P. L. Mattern, Opt. Commun. **30**, 249 (1979).
[9] Palmer, R. E., *The CARSFT Computer Code for Calculating Coherent Anti-Stokes Raman Spectra: User and Programmer Information*, Sandia National Laboratories Report SAND89-8206, Livermore, CA, 1989.
[10] J. Luque and D. R. Crosley, *LIFBASE: Database and Spectral Simulation Program (Version 1.5)*, SRI International Report MP 99-009, 1999.
[11] J. Laane and W. Kiefer, J. Raman Spectrosc. **9**, 353 (1980).
[12] W. Lempert, G. J. Rosasco, and W. S. Hurst, J. Chem. Phys. **81**, 4241 (1984).
[13] W. M. Huo, K. P. Gross, and R. L. McKenzie, Phys. Rev. Lett. **54**, 1012 (1985).
[14] T. Doerk, J. Ehlbeck, R. Jedamzik, J. Uhlenbusch, J. Höschele, and J. Steinwandel, Appl. Spectrosc. **51**, 1360 (1997).
[15] A. Pott, T. Doerk, J. Uhlenbusch, J. Ehlbeck, J. Höschele, and J. Steinwandel, J. Phys. D **31**, 2485 (1998).
[16] M. O. Scully, G. W. Kattawar, R. P. Lucht, T. Opatrný, H. Pilloff, A. Rebane, A. V. Sokolov, and M. S. Zubairy, Proc. Natl. Acad. Sci. U.S.A. **99**, 10994 (2002).